

From local to nonlocal high- Q plasmonic metasurfaces

Yao Liang,¹ Din Ping Tsai,^{1,2,3,*} and Yuri Kivshar^{4,†}

¹Department of Electrical Engineering, City University of Hong Kong, Hong Kong, China

²The State Key Laboratory of Terahertz and Millimeter Waves, City University of Hong Kong, Hong Kong, China

³Centre for Biosystems, Neuroscience and Nanotechnology, City University of Hong Kong, Hong Kong, China

⁴Nonlinear Physics Center, Research School of Physics, Australian National University, Canberra ACT 2615, Australia

The physics of bound states in the continuum (BICs) allows to design and demonstrate optical resonant structures with large values of the quality factor (Q -factor) by employing dielectric structures with low losses. However, BIC is a general wave phenomenon that should be observed in many systems, including the metal-dielectric structures supporting plasmons where the resonances are hindered by losses. Here we develop a comprehensive strategy to achieve high- Q resonances in plasmonic metasurfaces by effectively tailoring the resonant modes from local and nonlocal regimes.

Introduction—Recent progress in metaphotonics is driven by the physics of optical resonant modes supporting high values of the quality factor (Q -factor). One of the underpinning mechanisms for high- Q metaphotonics is associated with the physics of bound states in continuum (BICs) being known as spatially localized states residing in the continuum spectrum of extended states [1]. An ideal BIC is a dark state with infinite lifetime that in practice always turns into a quasi-BIC with finite lifetime [2]. The study of BICs and quasi-BICs has attracted a lot of attention in the recent years. The BIC concept has been employed for many problems requiring the enhancement of light-matter interaction with numerous applications including nanolasers [3, 4], high-harmonic generation [5], biosensing [6], optical imaging [7], etc.

In a majority of applications, BICs are realized in *dielectric photonic structures* fabricated of materials with high value of refractive index [6–9], and the underlying physics explores the idea to reduce the radiation Q factor by adjusting geometric parameters such as asymmetric of meta-atoms composing metasurfaces [2]. At the same time, several recent studies demonstrated the use of the BIC concept for plasmonic [10–12] and hybrid [13] structures.

The BIC concept relies of the basic principles of wave physics and wave interference [14]; therefore, it can be applied to both low-loss dielectric and high-loss plasmonics structures. Thus, the main question is: *What the general strategy for engineering high- Q resonances in plasmonic structures?* In this Letter, we uncover the basic physics of achieving high- Q plasmonic structures via the manipulation of dissipative properties of the resonant modes during the transition between local and nonlocal regimes in plasmonic metasurfaces.

Local to nonlocal transition in the parameter space—To illustrate our general strategy, first we focus on one recent example of a plasmonic metasurface (Fig. 1), consisting of vertical split-ring resonators (VSRs) on a golden film substrate [10]. This plasmonic structure supports dark and bright localized surface plasmon resonances (LSPRs). The initial geometric parameters are shown in the caption

of Fig. 2. By exclusively scaling the height parameters (the pillars and middle-connector heights) with the scaling factor α while keeping other parameters constant, it facilitates a transition between local and nonlocal regimes for both the modes. Here, $\alpha > 1$ indicates an increase, while $\alpha < 1$ signifies a decrease.

Figure 2 illustrates this transition in parameter space at $(k_x, k_y) = (0, 0)$, with k_x and k_y representing wave vector components along the x - and y -axes. We categorize even and odd symmetry LSPRs, corresponding to in-plane and out-of-plane resonances, as dark and bright modes based on their far-field radiation at local regimes. Decreasing the scaling parameter α from 1.5 to 0.01 leads to a shift from local to nonlocal resonance with 2 notable features: (1) the resonance wavelengths approach the period ($\lambda \rightarrow P$, where $P = 3\mu\text{m}$), as shown in Fig. 2c; (2) A significant increase in Q -factor (Fig. 2a), and mode volume (Fig. 2b) for both modes, with differences spanning several orders of magnitude.

In pure local regimes, when $\alpha = 1.5$, the bright LSPR mode, for example, exhibits a resonance wavelength ($\lambda \sim 10\mu\text{m}$) several times larger than the lattice period ($P = 3\mu\text{m}$), as shown in Fig. 2c. The individual

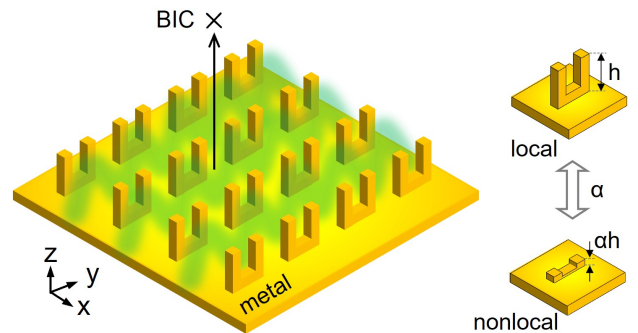


FIG. 1. Light-trapping in a plasmonic (gold) BIC metasurface with vertical split-ring resonators. Right: Scaling transition between local and nonlocal resonances through the parameter scaling, with α being the scaling parameter.

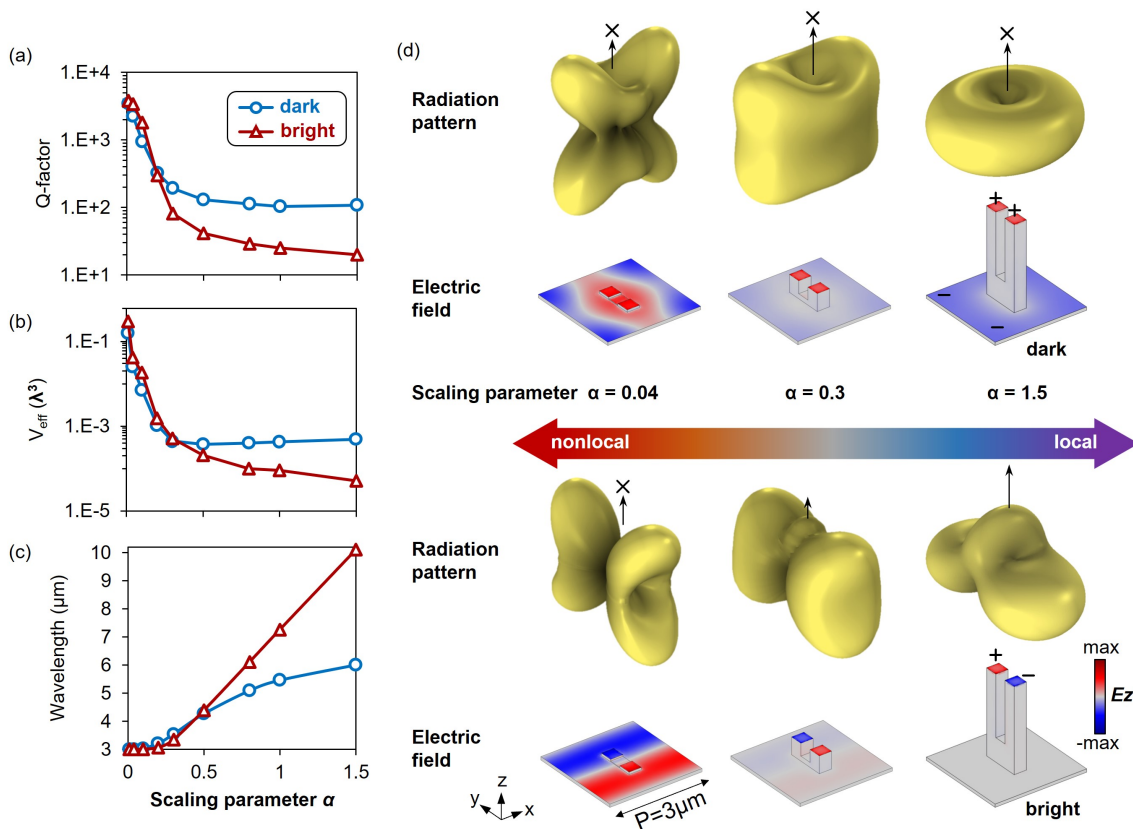


FIG. 2. Eigenmode analysis. (a)-(c) The Q -factor, mode volume, and resonance wavelength dependence on the scaling factor α for the dark and bright modes supported in the golden VSRR metasurface. The initial parameters (at $\alpha = 1$) are period $3 \mu\text{m}$, square pillar width $0.4 \mu\text{m}$ and high $1.8 \mu\text{m}$, middle connector height $0.5 \mu\text{m}$, center-to-center distance between pillars $0.8 \mu\text{m}$. (d) the radiation patterns and electric field (Ez) distributions during the transition between local and nonlocal regimes for various scaling factors.

unit resonance (local) prevails in this local LSPR, overshadowing negligible contributions from collective resonances (nonlocal) that depend on strong interactions among neighboring units [15]. This is evident because a single isolated unit exhibits a nearly identical electric field profile and spectral enhancement as the entire array. (Supplemental Material (SM) [16], S3).

However, the Q -factor for the bright LSPR is low, $Q \approx 19.8$ at $\alpha = 1.5$ (Fig. 2a). This is predominantly attributed to two reasons.

First, its tight light confinement, evident through hotspots on the tops of pillars (Fig. 2d) and an ultra-small mode volume well below the diffraction limit ($V_{eff} \sim 5.13 \times 10^{-5} \lambda^3$, Fig. 2b). These hotspots amplify the electric field ($|\mathbf{E}|$), causing a notable increase in the metal's dissipation density, $w = 1/2\epsilon_0 \Im(\epsilon) |\mathbf{E}|^2$, where ϵ_0 and $\epsilon = \epsilon_r + i\epsilon_i$ denote the vacuum permittivity and relative permittivity of gold. This giant dissipation loss hampers sustaining light energy exchange between the E-field and the H-field, preventing high- Q resonances. The reason is simple: high- Q resonances, known for long-lasting light oscillation in cavities, require a sustaining oscillation between electric field energy ($u_E \propto \epsilon E^2$) and

magnetic field energy ($u_H \propto \mu H^2$) in a cavity due to light's electromagnetic nature, where μ is the permeability [17]; Once giant E-field or H-field hotspots present, this oscillation is damaged, leading to low- Q resonances.

Second, it has giant radiation loss. In plasmonic cavities, their resonance Q -factor reads

$$Q^{-1} = Q_{rad}^{-1} + Q_{dis}^{-1} \quad (1)$$

where Q_{rad} and Q_{dis} are, respectively, the radiation and dissipation Q -factors. See SM [16], S1 for simulation/calculation details.

One way to improve the LSPR Q -factor is to suppress radiation loss using dark modes without radiation loss, $Q_{rad} = \infty$. The Q -factor for the dark LSPR is $Q \approx 107.8$ at $\alpha = 1.5$ (Fig. 2a), representing a $5\times$ improvement over the bright LSPR. However, the Q -factor of the dark LSPR is still limited by the giant dissipation loss, as it has hotspots on pillars tops (Fig. 2d).

Using our local-to-nonlocal transition strategy is an effective way to minimize dissipation loss. In this transition, the E-field becomes less confined and extends more into the lossless air (SM[16], S4). This is accomplished by increasing mode volumes (Fig. 2b) and the gradual

disappearance of hotspots on pillar tops, eventually resulting in a uniformly distributed E-field profile on the gold film plane (Fig. 2d). These two features substantially reduce resonances' dissipation loss, as indicated by large Q-factors, $Q \approx 3439$ (dark) and $Q \approx 3802$ (bright) at $\alpha = 0.01$ for both modes (Fig. 2a), several orders of magnitude larger than the local LSPRs.

Diffraction orders and nonlocality—Plasmonic resonance modes in a periodic array can be decomposed into Bloch harmonics [18], given by $\mathbf{E}(\mathbf{r}) = \sum a_{(p,q)} e^{-i(\mathbf{G} + k_{\parallel})\mathbf{r}}$, where $a_{(p,q)}$ is the complex amplitude, $k_{\parallel} = k_x + k_y$ the in-plane k-vector, $\mathbf{G} = 2\pi p/P_x + 2\pi q/P_y$ the array reciprocal vector, with the meta-unit periods $P_x = P_y = P$ and $p, q \in \mathbb{Z}$. We identify a highly symmetric position $(k_{\parallel}, \lambda) = (0, \lambda_D)$ in momentum space as the D point, where several diffraction orders degenerate, such as $(p, q) = (+1, 0)$, $(+1, 0)$, $(0, \pm 1)$, and $\lambda_D = P$ is the degenerate wavelength.

Interestingly, D point ($\lambda = \lambda_D$) is a critical transition point, where the Bloch harmonics $(+1, 0)$, $(+1, 0)$, $(0, \pm 1)$ can either be stored as bounded evanescent waves when $|G| > |2\pi/\lambda|$ ($|G| = 2\pi/P$ and $\lambda > \lambda_D$), or become propagating diffraction orders when $\lambda < \lambda_D$. We involve normalized detuning wavelength (Δ) to describe the distance between resonance wavelength (λ) and λ_D

$$\Delta = \frac{\lambda - \lambda_D}{\lambda_D} \quad (2)$$

As Δ decreases and approaches 0, the LSPRs (strong light confinement) gradually turn into surface plasmon polaritons (SPPs) with E-field enormously extending into the air due to their strong coupling with the nonlocal diffraction orders. This explains why the nonlocal modes have mode volumes orders of magnitude bigger than the local LSPRs (Fig. 2).

Nonlocal modes nature—The high- Q nonlocal modes are trapped SPPs, characterized by standing SPP waves confined in a Fabry-Pérot cavity (SM [16], S4, S5). Two pieces of evidence support this interpretation.

First, trapped SPPs exhibit no far-field radiation. Consequently, all nonlocal plasmonic modes, whether transitioning from a dark or bright LSPR in the local to nonlocal shift, should remain sub-radiative if they are trapped SPPs. The dark LSPR supports this characteristic throughout the transition (Fig. 2d). Interestingly, despite being radiative in local regimes ($\alpha = 1.5$), the bright LSPR becomes less radiative as α decreases to 0.3 and eventually becomes radiation-free in nonlocal regimes ($\alpha \leq 0.04$) (see Fig. 2d and S3 in SM[16]). This alignment with the dark feature of trapped SPPs. Second, another evidence is linked to the Q-factor limit of the nonlocal mode.

Q-factor limit—As Δ decreases, dark and bright LSPRs shift into trapped SPPs, exhibiting minimal dissipation loss, enabling efficient energy exchange between E-field and H-field. To determine the upper limit of Q-

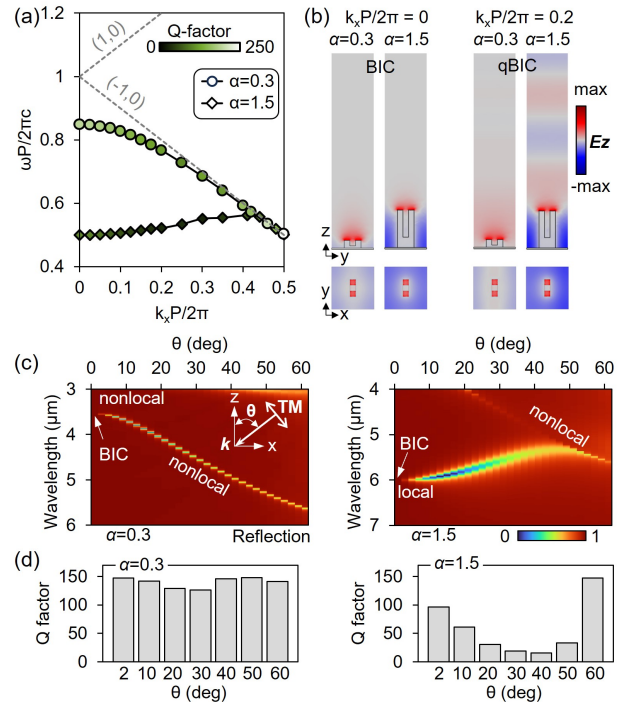


FIG. 3. (a) Calculated band structure for the dark mode with nonlocal ($\alpha = 0.3$) and local ($\alpha = 1.5$) characteristics, denoted by circular and square markers, respectively. The color represents eigenmode Q-factor. The gray dashed lines represent two diffraction orders, $(+1, 0)$ and $(-1, 0)$. (b) The field distribution of dark modes for two metasurfaces ($\alpha = 0.3$ and $\alpha = 1.5$) at $k_x P/2\pi = 0$ (Γ point) and $k_x P/2\pi = 0.2$ (off- Γ). (c) Reflection spectra for two metasurfaces ($\alpha = 0.3$ and $\alpha = 1.5$) at oblique incidence in the x-z plane. (d) The corresponding Q-factor of the two dark modes at different oblique angles.

factors for nonlocal plasmonic resonances we can assess:

$$Q_{max} = k_{spp}^r / 2k_{spp}^i \quad (3)$$

where k_{spp}^r and k_{spp}^i are the real and imaginary part of SPPs k-vector, such that $k_{spp} = k_{spp}^r + ik_{spp}^i = \frac{2\pi}{\lambda} \sqrt{\frac{\epsilon\epsilon_0}{\epsilon + \epsilon_0}}$, where ϵ and ϵ_0 are the permittivities of gold and vacuum [19]. As ϵ varies with wavelength, the maximum Q-factor of nonlocal plasmonic resonance is wavelength-dependent (SM [16], S5). For $\lambda \approx 3\mu\text{m}$, the trapped SPPs Q-factor is calculated as ~ 3805 , consistent with numerical results of nonlocal mode in Fig. 2a.

Local-nonlocal transition in the momentum space—The local-to-nonlocal transition can also occur in the momentum space as the resonance modes interact with nonlocal diffraction orders. For example, we calculate the eigenfrequency and Q-factor for two dark modes with different height parameters, $\alpha = 1.5$ (local) and $\alpha = 0.3$ (nonlocal), as shown in Fig. 3a. They both symmetry-protected BICs with zero radiation loss at the Γ -point ($k_{\parallel} = 0$), as shown in Fig. 2b (left). As the in-plane vector k_x increases, BICs transit to quasi-BICs with several distinguished properties:

First, the Q-factor of the local quasi-BIC mode experiences a rapid decrease, whereas the Q-factor of the nonlocal quasi-BIC mode remains stable, as verified by both eigenmode studies (Fig. 3a) and full-wave simulations (Figs. 3c,d). This can be explained in terms of coupling strength between the resonance modes and nonlocal diffraction order $(-1, 0)$. For example, the local mode is closer to the $(-1, 0)$ with a smaller Δ than its nonlocal counterpart at $k_x P/2\pi = 0.2$. Thus, it relies more on the mutual interaction among neighboring units, which reduces its radiation loss [15]. This makes it less radiative compared to the local counterpart (Fig. 3b, right). Also, its nonlocal feature makes it less dissipative. These two features help it keep high-Q resonances at various oblique incidences (Fig. 3c,d).

Second, the local mode becomes nonlocal at large oblique incidence angles ($\theta > 40^\circ$) as the detuning wavelength decreases. This is evident by a sudden increase in its Q-factor when $\theta > 40^\circ$ (Fig. 3d).

Local-nonlocal transition in plasmonic metasurfaces—Our approach to enhancing the Q-factor in plasmonic nanostructures by reducing the height parameter is not limited to a specific metasurface with VSRR units. Instead, it is a universally applicable strategy that can be employed for all types of plasmonic metasurfaces with various meta-units, including single pillar, ring, dimmer, verticle triangle, pillar-wall, and many others [10–12, 20–27], as shown in Fig. 4.

All meta-atoms in Fig. 4 can support LSPRs. For simplicity in our discussion, we set them square units with a period of $3\mu\text{m}$, and their initial height as $1.8\mu\text{m}$ (at $\alpha = 1$). Thus, their degenerate wavelength, where $(+1, 0)$, $(+1, 0)$, $(0, \pm 1)$ diffraction orders emerge, is $\lambda_D = 3\mu\text{m}$. As the height scaling parameter α decreases, the LSPRs (dark or bright) begin to transition into trapped SPPs with similar E-field profiles, whether exhibiting symmetry or anti-symmetry (SM [16], S7).

We study the dependence of the dissipation Q-factor Q_{dis} on the normalized detuning wavelength Δ for all plasmonic metasurfaces during the local (LSPRs) to nonlocal (trapped SPPs) transition (Fig. 4). An inverse square root law well approximates the relationship

$$Q_{dis} \propto \frac{1}{\sqrt{\Delta}} \quad (4)$$

where Δ is calculated using Eq. 2, and the dissipation Q-factor using Eq. 1 (SM [16], S1). Notably, in the non-local regimes ($\alpha \sim 10^{-3}$), the Q-factor ($Q = Q_{dis}$) of all plasmonic metasurfaces is approaching ~ 3800 , consistent with prediction using Eq. 3, confirming the trapped SPPs nature of the nonlocal modes.

Although drawing a clear line between local and non-local regimes is difficult, the inverse square root law suggests an intelligent way to engineer plasmonic structures with on-demand resonances during this transition. For example, most resonances have hybrid (LSPRs + SPPs) properties during the local-to-nonlocal transition. For

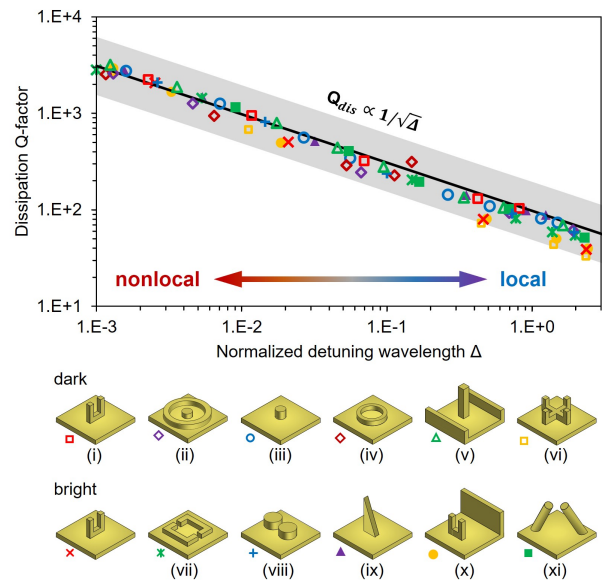


FIG. 4. Dependence of the dissipation Q factor on the normalized detuning wavelength Δ (log-log scale) for various all-plasmonic designs [(i) to (xi)] supports bright/dark LSPRs (Refs. [10–12, 20–27]). All square units have a $3\mu\text{m}$ period.

example, at $\alpha = 0.3$, the bright mode has both hotspots (local) on pillars tops and trapped SPPs on the ground plane (Fig. 2d). Notably, hotspots [28] and high-Q resonances [10] are effective ways to enhance the electromagnetic field. Consequently, the maximum E-field intensity occurs at some point during this transition (SM [16], S3), which proves beneficial for applications such as nonlinear enhancement [29].

Equation (4) is valid for a broad range, $\Delta \in [10^{-3}, 1]$, allowing diverse Q-factor choices for most plasmonic metasurfaces, ranging from tens to thousands. However, the plasmonic Q-factor has inherent limits, approaching that of trapped SPPs (Eq. 3). To attain higher Q-factors, selecting a longer operational wavelength is crucial, as the maximum Q-factor is wavelength-dependent. This is exemplified by $Q_{max} \sim 627$ at $\lambda = 880\text{nm}$ and $Q_{max} \sim 6330$ at $\lambda = 5\mu\text{m}$ (SM [16], S6). This wavelength-dependent trend aligns with recent experimental findings (~ 80 in near-IR [20] and ~ 500 in mid-IR [30])

Conclusion—We have suggested and demonstrated a general conceptual approach for achieving large Q factors in plasmonic metasurfaces by engineering dissipative losses and dissipation Q factor of the resonant modes. Our approach employs plasmonic local and extended resonances based on the BIC physics, and it is underpinned by an efficient control of local and nonlocal optical response. We believe our approach opens the door to many applications of high- Q plasmonic structures including subwavelength lasers, harmonic generation, biosensing, optical imaging, entangled photon generation, etc.

This work is supported by the University Grants

Committee / Research Grants Council of the Hong Kong Special Administrative Region, China [Project No. AoE/P-502/20, CRF Project: C1015-21E; C5031-22G; and GRF Project: CityU15303521; CityU11305223; CityU11310522; CityU11300123], the Department of Science and Technology of Guangdong Province [Project No. 2020B1515120073], City University of Hong Kong [Project No. 9380131, 9610628, and 7005867], and the Australian Research Council (grant DP210101292).

* dptsai@cityu.edu.hk

† yuri.kivshar@anu.edu.au

- [1] C. W. Hsu, B. Zhen, A. D. Stone, J. D. Joannopoulos, and M. Soljačić, Bound states in the continuum, *Nature Reviews Materials* **1**, 1 (2016).
- [2] K. Koshelev, S. Lepeshov, M. Liu, A. Bogdanov, and Y. Kivshar, Asymmetric metasurfaces with high-q resonances governed by bound states in the continuum, *Physical Review Letters* **121**, 193903 (2018).
- [3] A. Kodigala, T. Lepetit, Q. Gu, B. Bahari, Y. Fainman, and B. Kanté, Lasing action from photonic bound states in continuum, *Nature* **541**, 196 (2017).
- [4] M.-S. Hwang, H.-C. Lee, K.-H. Kim, K.-Y. Jeong, S.-H. Kwon, K. Koshelev, Y. Kivshar, and H.-G. Park, Ultralow-threshold laser using super-bound states in the continuum, *Nature Communications* **12**, 4135 (2021).
- [5] G. Zograf, K. Koshelev, A. Zalogina, V. Korolev, R. Hollinger, D.-Y. Choi, M. Zuerch, C. Spielmann, B. Luther-Davies, D. Kartashov, *et al.*, High-harmonic generation from resonant dielectric metasurfaces empowered by bound states in the continuum, *ACS Photonics* **9**, 567 (2022).
- [6] A. Leitis, A. Tittl, M. Liu, B. H. Lee, M. B. Gu, Y. S. Kivshar, and H. Altug, Angle-multiplexed all-dielectric metasurfaces for broadband molecular fingerprint retrieval, *Science Advances* **5**, eaaw2871 (2019).
- [7] F. Yesilkoy, E. R. Arvelo, Y. Jahani, M. Liu, A. Tittl, V. Cevher, Y. Kivshar, and H. Altug, Ultrasensitive hyperspectral imaging and biodetection enabled by dielectric metasurfaces, *Nature Photonics* **13**, 390 (2019).
- [8] Z. Chen, X. Yin, J. Jin, Z. Zheng, Z. Zhang, F. Wang, L. He, B. Zhen, and C. Peng, Observation of miniaturized bound states in the continuum with ultra-high quality factors, *Science Bulletin* **67**, 359 (2022).
- [9] J. Jin, X. Yin, L. Ni, M. Soljačić, B. Zhen, and C. Peng, Topologically enabled ultrahigh-q guided resonances robust to out-of-plane scattering, *Nature* **574**, 501 (2019).
- [10] Y. Liang, K. Koshelev, F. Zhang, H. Lin, S. Lin, J. Wu, B. Jia, and Y. Kivshar, Bound states in the continuum in anisotropic plasmonic metasurfaces, *Nano Letters* (2020).
- [11] Y. Liang, H. Lin, S. Lin, J. Wu, W. Li, F. Meng, Y. Yang, X. Huang, B. Jia, and Y. Kivshar, Hybrid anisotropic plasmonic metasurfaces with multiple resonances of focused light beams, *Nano Letters* **21**, 8917 (2021).
- [12] A. Aigner, A. Tittl, J. Wang, T. Weber, Y. Kivshar, S. A. Maier, and H. Ren, Plasmonic bound states in the continuum to tailor light-matter coupling, *Science Advances* **8**, eadd4816 (2022).
- [13] S. I. Azzam, V. M. Shalaev, A. Boltasseva, and A. V. Kildishev, Formation of bound states in the continuum in hybrid plasmonic-photonic systems, *Physical Review Letters* **121**, 253901 (2018).
- [14] K. L. Koshelev, Z. F. Sadrieva, A. A. Shcherbakov, Y. S. Kivshar, and A. A. Bogdanov, Bound states of the continuum in photonic structures, *Physics-Uspekhi* **66**, 494 (2023).
- [15] V. G. Kravets, A. V. Kabashin, W. L. Barnes, and A. N. Grigorenko, Plasmonic surface lattice resonances: a review of properties and applications, *Chemical Reviews* **118**, 5912 (2018).
- [16] Supplemental Material: Simulation details, mode volume calculation, single particle resonances VS array resonances, dissipation loss control during the transition between local and nonlocal regimes, trapped SPPs, dissipation Q-factor limit of Trapped SPPs, and local and nonlocal transition for various plasmonic metasurfaces, which includes more Refs.[31–42].
- [17] J. B. Khurgin, How to deal with the loss in plasmonics and metamaterials, *Nature Nanotechnology* **10**, 2 (2015).
- [18] R. Engelen, D. Mori, T. Baba, and L. Kuipers, Subwavelength structure of the evanescent field of an optical Bloch wave, *Physical Review Letters* **102**, 023902 (2009).
- [19] A. V. Zayats, I. I. Smolyaninov, and A. A. Maradudin, Nano-optics of surface plasmon polaritons, *Physics Reports* **408**, 131 (2005).
- [20] A. Yang, Z. Li, M. P. Knudson, A. J. Hryn, W. Wang, K. Aydin, and T. W. Odom, Unidirectional lasing from template-stripped two-dimensional plasmonic crystals, *ACS Nano* **9**, 11582 (2015).
- [21] A. E. Cetin and H. Altug, Fano resonant ring/disk plasmonic nanocavities on conducting substrates for advanced biosensing, *ACS Nano* **6**, 9989 (2012).
- [22] B. Gerislioglu, L. Dong, A. Ahmadvand, H. Hu, P. Nordlander, and N. J. Halas, Monolithic metal dimer-on-film structure: New plasmonic properties introduced by the underlying metal, *Nano Letters* **20**, 2087 (2020).
- [23] Z. Li, S. Butun, and K. Aydin, Ultranarrow band absorbers based on surface lattice resonances in nanostructured metal surfaces, *ACS Nano* **8**, 8242 (2014).
- [24] Z. Shen, X. Fang, S. Li, W. Yin, L. Zhang, and X. Chen, Terahertz spin-selective perfect absorption enabled by quasi-bound states in the continuum, *Optics Letters* **47**, 505 (2022).
- [25] Y. Tang, Y. Liang, J. Yao, M. K. Chen, S. Lin, Z. Wang, J. Zhang, X. G. Huang, C. Yu, and D. P. Tsai, Chiral bound states in the continuum in plasmonic metasurfaces, *Laser & Photonics Reviews* **17**, 2200597 (2023).
- [26] X. Xiong, S.-C. Jiang, Y.-H. Hu, R.-W. Peng, and M. Wang, Structured metal film as a perfect absorber, *Advanced Materials* **25**, 3994 (2013).
- [27] P. Zilio, M. Malerba, A. Toma, R. P. Zaccaria, A. Jacassi, and F. D. Angelis, Hybridization in three dimensions: a novel route toward plasmonic metamolecules, *Nano Letters* **15**, 5200 (2015).
- [28] D. Tsai, J. Kovacs, Z. Wang, M. Moskovits, V. M. Shalaev, J. Suh, and R. Botet, Photon scanning tunneling microscopy images of optical excitations of fractal metal colloid clusters, *Physical Review Letters* **72**, 4149 (1994).
- [29] R. Czaplicki, A. Kiviniemi, M. J. Huttunen, X. Zang, T. Stolt, I. Vartiainen, J. Butet, M. Kuittinen, O. J. Martin, and M. Kauranen, Less is more: Enhancement of second-harmonic generation from metasurfaces by reduced nanoparticle density, *Nano Letters* **18**, 7709 (2018).
- [30] S.-Q. Li, W. Zhou, D. Bruce Buchholz, J. B. Ketterson, L. E. Ocola, K. Sakoda, and R. P. Chang, Ultra-sharp

- plasmonic resonances from monopole optical nanoantenna phased arrays, *Applied Physics Letters* **104** (2014).
- [31] R. L. Olmon, B. Slovick, T. W. Johnson, D. Shelton, S.-H. Oh, G. D. Boreman, and M. B. Raschke, Optical dielectric function of gold, *Physical Review B* **86**, 235147 (2012).
- [32] S. A. Maier, Plasmonic field enhancement and sers in the effective mode volume picture, *Optics Express* **14**, 1957 (2006).
- [33] J. R. Krenn, A. Dereux, J.-C. Weeber, E. Bourillot, Y. Lacroute, J.-P. Goudonnet, G. Schider, W. Gotschy, A. Leitner, F. R. Aussenegg, *et al.*, Squeezing the optical near-field zone by plasmon coupling of metallic nanoparticles, *Physical Review Letters* **82**, 2590 (1999).
- [34] R. W. Wood, Xlii. on a remarkable case of uneven distribution of light in a diffraction grating spectrum, *The London, Edinburgh, and Dublin Philosophical Magazine and Journal of Science* **4**, 396 (1902).
- [35] W. Zhou and T. W. Odom, Tunable subradiant lattice plasmons by out-of-plane dipolar interactions, *Nature Nanotechnology* **6**, 423 (2011).
- [36] P. Zijlstra, P. M. Paulo, and M. Orrit, Optical detection of single non-absorbing molecules using the surface plasmon resonance of a gold nanorod, *Nature Nanotechnology* **7**, 379 (2012).
- [37] N. Liu, M. Mesch, T. Weiss, M. Hentschel, and H. Giessen, Infrared perfect absorber and its application as plasmonic sensor, *Nano Letters* **10**, 2342 (2010).
- [38] M. S. Bin-Alam, O. Reshef, Y. Mamchur, M. Z. Alam, G. Carlow, J. Upham, B. T. Sullivan, J.-M. Ménard, M. J. Huttunen, R. W. Boyd, *et al.*, Ultra-high-q resonances in plasmonic metasurfaces, *Nature Communications* **12**, 974 (2021).
- [39] X. Yu, L. Shi, D. Han, J. Zi, and P. V. Braun, High quality factor metallodielectric hybrid plasmonic–photonic crystals, *Advanced Functional Materials* **20**, 1910 (2010).
- [40] R. W. Wood, Anomalous diffraction gratings, *Physical Review* **48**, 928 (1935).
- [41] T. Joshua and H. Ong, Quality factor of plasmonic monopartite and bipartite surface lattice resonances, *Physical Review B* **104**, 125442 (2021).
- [42] A. Sobhani, A. Manjavacas, Y. Cao, M. J. McClain, F. J. García de Abajo, P. Nordlander, and N. J. Halas, Pronounced linewidth narrowing of an aluminum nanoparticle plasmon resonance by interaction with an aluminum metallic film, *Nano Letters* **15**, 6946 (2015).